Calcif Tissue Int (2010) 87:273–283
DOI 10.1007/s00223-010-9395-7

A Rationale for Osteoclast Selectivity of Inhibiting the Lysosomal V-ATPase a3 Isoform

Jonas K. E. Nyman · H. Kalervo Väänänen

Received: 22 March 2010 / Accepted: 9 June 2010 / Published online: 2 July 2010

Abstract Osteoclastic bone resorption can be completely abolished by inhibiting the vacuolar H^+-ATPase (V-ATPase), a proton pump composed of at least 12 different subunits. However, V-ATPases are ubiquitous and it is unclear whether the osteoclast V-ATPase has a unique composition that would allow its selective inhibition. Aiming to answer this question, we compared human osteoclasts and monocytic THP.1 cells with respect to the localization of the a3 isoform of the 116-kDa subunit, which is indispensable for bone resorption, and sensitivity to SB242784, a V-ATPase inhibitor that prevents experimentally induced osteoporosis. By immunofluorescence, a3 was essentially nondetectable in THP.1 cells, while in osteoclasts a3 was highly upregulated and localized to lysosomes in nonresorbing osteoclasts. We isolated the lysosomal compartment from both sources as latex bead-containing phagolysosomes and compared them. Osteoclast phagolysosomes and THP.1 phagolysosomes both contained a3 and a1; however, the a3/a1 ratio was 3.8- to 11.2-fold higher in osteoclast phagolysosomes. Importantly, the V-ATPase-dependent acidification of phagolysosomes from both sources was essentially equally sensitive to SB242784. Thus, we observed no indication of a qualitative uniqueness of the osteoclast V-ATPase; rather, the high a3-level in osteoclasts may represent an upregulation of the common lysosomal V-ATPase. Our results, together with the reported phenotype of a3 deficiency and the reported efficacy of SB242784 in vivo, suggest that V-ATPase structure-independent mechanisms render bone resorption more sensitive than lysosomal function to V-ATPase inhibition. One such mechanism may be compensation of a3 by a1, which may be sufficient for retaining lysosomal function but not bone resorption.

Keywords Osteoclast · V-ATPase · Phagolysosome · Acidification · Osteoporosis

Osteoclastic resorption of bone is accomplished by dissolution of bone mineral by targeted secretion of protons into the resorption lacuna and subsequent enzymatic hydrolysis of the organic matrix. The acid secretion is driven by the vacuolar H^+-ATPase (V-ATPase), a 560-kDa protein composed of at least 12 different subunits, and accompanied by passive chloride flow through chloride channels. Bone resorption in vitro can be completely inhibited by low concentrations of V-ATPase inhibitors [1], and V-ATPase is an obvious drug target for diseases resulting from increased bone resorption, such as postmenopausal osteoporosis. However, V-ATPases acidify many different cell organelles; and thus, V-ATPases are mediators of many basic cell functions (review in [2]). The most potent V-ATPase inhibitors, the macrolid antibiotics bafilomycins and concanamycins, are not useful as drugs for osteoporosis since in vivo they are toxic at doses that are needed to inhibit bone resorption [3]. Therefore, inhibitor selectivity for the osteoclast V-ATPase is needed before a therapeutic approach is possible.

Although synthetic analogues of the macrolid V-ATPase inhibitors are potent and showed differential selectivity between microsomal V-ATPase activity from different tissues [4–6] and were effective in rat models of bone loss

The authors have stated that they have no conflict of interest.

J. K. E. Nyman (✉) · H. K. Väänänen
Department of Cell Biology and Anatomy, Institute of Biomedicine, University of Turku, Kiinamyllynkatu 10, 20520 Turku, Finland
e-mail: jonnym@utu.fi

[7], the rationale for such selectivity is yet poorly understood. At least two principal obstacles have contributed to this fact: the complexity of the osteoclast and that of the V-ATPase itself. With the cloning of different isoforms of the V-ATPase subunits progress has recently been made. One potential mediator of inhibitor selectivity is the transmembrane 116-kDa subunit, out of which four isoforms have been cloned [8–10]. These isoforms are differentially expressed, and they differ more from each other than the isoforms of the other subunits. Isoforms a1, a2, and a3 were shown to be expressed in osteoclasts [9, 11], while isoform a4 expression may be restricted to intercalated cells in kidney cortex [10] and epithelial cells of the endolymphatic sac [12]. While there are few data concerning the expression of the isoforms of the other subunits in osteoclasts, accumulating evidence has shown that the a3 isoform, which is expressed at high levels in osteoclasts [13], is indispensable for proper bone resorption as knockout of the a3 gene in mice results in a severe osteopetrotic phenotype [14] and, in humans, mutations in the corresponding gene are a common cause of infantile malignant osteopetrosis [15–18]. However, by RT-PCR a3 mRNA has been found in all tested cell lines and tissues [19], indicating ubiquitous expression of a3 and questioning whether osteoclast-selective V-ATPase inhibition may be achieved by targeting the a3 isoform. Still, it remains to be elucidated whether the osteoclast V-ATPase indeed has any unique features that would enable selective inhibition.

We analyzed the rationale for the V-ATPase of the osteoclast as a drug target. First, we analyzed the subcellular localization of a3 in in vitro differentiated human osteoclasts. Second, we showed that the isoform a3-containing vesicular compartment from osteoclasts can be isolated as phagolysosomes. The isolated compartment was compared with the corresponding compartment from a monocytic cell line with respect to the acidifying properties, including sensitivity to bafilomycin A1 and SB242784, the latter being selective between V-ATPases from different tissues [4] and reported to be osteoclast-selective [7]. In light of our results, we propose mechanisms by which a3-selective inhibition may be selective for bone resorption, despite ubiquitous a3 expression.

Materials and Methods

Cells and Media

Human osteoclasts were cultured from peripheral blood monocytes from male blood donors essentially as described previously [20]. Briefly, the monocyte- and leucocyte-rich fraction was separated from erythrocytes and polymorphonuclear cells by Ficoll centrifugation. After washing the cells in PBS, they were suspended to 20 million/ml α-MEM and plated at a density of 20,000/mm^2 either on thin slices of bovine cortical bone, glass coverslips, or tissue culture wells, depending on the experiment. After 2 h, nonadherent cells were removed by gentle swirling of the plate, and adherent cells were induced to differentiate to osteoclasts by culturing in α-MEM supplemented with 10% inactivated fetal bovine serum, 20 ng/ml RANK-L (PeproTech, Rocky Hill, NJ), 10 ng/ml macrophage-colony stimulating factor (PeproTech), and 10 nM dexamethasone and penicillin–streptomycin. Half of the medium was changed every third or fourth day. This protocol generated multinucleated osteoclasts with varying portions of nonosteoclastic mononuclear cells. Before performing the experiments with latex beads, the purity of osteoclast cultures was increased by trypsin treatment to detach mononuclear cells, and the resulting purity of these osteoclast cultures was >95% (osteoclast nuclei/nuclei of mononuclear cells). The THP.1 monocyte cell line was cultured in RPMI-1640 supplemented with 10% inactivated fetal bovine serum, 5 mM HEPES, 1 mM sodium pyruvate, and penicillin–streptomycin. In all experiments, THP.1 cells were induced to more actively phagocytosing macrophages by treatment with 10 ng/ml phorbol-12-myristate-13-acetate (PMA) for 16 h and cultured for additional 24 h in the absence of PMA and HEPES before use in the experiments with latex beads. Where indicated, THP.1 cells were treated with 20 μM cytochalasin D.

Chemicals

SB242784, (2Z,4E)-5-(5,6-dichloro-2-indolyl)-2-methoxy-*N*-(1,2,2,6,6-pentamethylpiperidin-4-yl)-2,4-pentadienamide [4], was synthesized and kindly provided by Terrence Kee (Leeds, UK). Unless otherwise indicated, all other chemicals were from Sigma-Aldrich (St. Louis, MO).

Antibodies

Two different human V-ATPase isoform a3 peptide-specific antisera were used in this study. One, provided by Professor John Findlay (Leeds UK), was raised against a peptide corresponding to amino acids 661–691 and the other, raised against a peptide corresponding to the carboxy terminus (amino acids 811–829), was provided by Dr. Jan Mattsson, as was the antibody against subunit A [15]. Mouse monoclonal antibodies used in the immunocytostaining experiments were against lysosome-associated membrane protein-2 (LAMP-2) (Research Diagnostics, Minneapolis, MN), cathepsin K (Fuji Chemicals, Tokyo, Japan), early endosomal antigen-1 (Transduction Laboratories, Lexington, KY), Rab11 (Transduction Laboratories), matrix metalloproteinase-9 (NeoMarkers, Fremont,

CA), and osteocalcin (3H9, 3H8, 8H12) [21]. Secondary antibodies used in the immunocytostaining studies were either fluorescein isothiocyanate- or tetramethylrhodamine isothiocyanate-conjugated donkey anti-mouse or donkey anti-rabbit (Jackson ImmunoResearch Laboratories, West Grove, PA). The antibodies recognizing V-ATPase a1 and Rab7 were purchased from Santa Cruz Biotechnology (Santa Cruz, CA). The production of antisera against cytoplasmic carbonic anhydrase II [22] and mitochondrial carbonic anhydrase V [23] has been described. The horseradish peroxidase-conjugated secondary antibodies used in immunoblotting were purchased from Zymed (San Francisco, CA).

Immunostaining and Microscopy

Cells were briefly rinsed in PBS, fixed for 20 min in 3% paraformaldehyde, and permeabilized in ice-cold acetone for 30 s. Cells were incubated in PBS containing 2% bovine serum albumin for 30 min to block unspecific binding. Staining was performed by sequential 1-h incubations with primary and fluorochrome-conjugated secondary antibodies diluted in PBS containing 0.5% bovine serum albumin, separated by four washes with PBS, 5 min each. When fluorochrome-conjugated phalloidin was used to stain filamentous actin, it was included in the solution containing the secondary antibody. After counterstaining of nuclei with Hoechst and three 5-min washes, samples were mounted on microscope slides and viewed under a Leica (Heidelberg, Germany) confocal microscope or an Olympus (Tokyo, Japan) fluorescence microscope.

Immunoblotting

For whole-cell lysates, THP.1 cells and osteoclasts were collected into lysis buffer (1% Triton X-100, 10 mM Tris–HCl [pH 7.5], 1 mM EDTA, 50 mM NaCl, protease inhibitor cocktail [Complete Mini; Roche, Indianapolis, IN]) and briefly sonicated to fragment DNA. The protein concentration was determined using Bradford reagent, and a 5× sample buffer (10% SDS, 300 mM TrisCl [pH 6.8] 0.4% bromophenol blue, 50% glycerol) was added to the samples before 10 μg protein per sample were separated with SDS-PAGE. For immunoblotting of the latex bead-containing phagolysosomes from osteoclasts and THP.1 cells, isolated phagolysosomes were collected by centrifugation and 5× sample buffer was added to the pellets. Out of these samples, aliquots that contained approximately as much LAMP-2 as did 10 μg of the parental whole-cell lysates were loaded. After SDS-PAGE, the separated peptides were transferred to nitrocellulose membrane (Bio-Rad, Richmond, CA) with a semidry transfer system. Unspecific binding was blocked by incubating the membrane for 1 h in PBS containing 5% skim milk. Primary antibodies, diluted in PBS containing 3% skim milk and 0.3% Tween-20, were incubated overnight at 4°C. On the next day, membranes were washed four times for 5 min each time with PBS containing 0.3% Tween-20 and incubated for 1 h with PBS containing secondary antibody, 2% skim milk, and 0.3% Tween-20. After four washes, 5 min each, in PBS containing 0.3% Tween-20, bands were detected with Immun-Star reagents (Bio-Rad) and X-ray film (Kodak, Rochester, NY).

Isolation of Chicken Bone and Brain Microsomes

Regular egg-laying hens, housed by the University of Turku, were killed and the medullary bone from the femora and tibiae was collected into an isolation buffer (250 mM sucrose, 1 mM EGTA, 1 mM $NaHCO_3$, 10 mM Tris–HCl [pH 7.0], 1 mM dithiothreitol, and protease inhibitor cocktail [Complete Mini]). After brief homogenization in Ultra Turrax, the tissue was further homogenized with a glass–glass dounce homogenizator. Pieces of bone, unbroken cells, mitochondria, and nuclei were pelleted by centrifugation of the homogenate for 15 min at $10{,}000\times g$, and the resulting supernatant was subjected to ultracentrifugation at $100{,}000\times g$ for 45 min. The final pellet was dissolved in isolation buffer and frozen at −70°C until used. Brain microsomes were prepared according to the same protocol, except that chicken cerebrum and cerebellum were used as the starting material.

Isolation of Phagolysosomes with Latex Beads

The protocol was essentially adapted from a previously described one [24] with some modifications. Blue-colored latex beads, 0.8 μm in diameter (Sigma-Aldrich), were diluted 1:100 in the appropriate medium just enough to cover the cells for the 4-h pulse time. Nonphagocytosed latex beads were removed by rinsing the cells with PBS until few free-floating beads were visible under the microscope. After the chase time, the medium was exchanged for ice-cold isolation buffer, and the cells were scraped off the plates and homogenized in a glass–glass dounce homogenizator. By adding isolation buffer containing 60% sucrose, the sucrose content of the homogenized solution was adjusted to 34% (w/w) and loaded under a sucrose gradient of 10, 20, 25, and 30% (top to bottom). After ultracentrifugation at $100{,}000\times g$ for 90 min, phagolysosomes were collected from the 10–20% interphase. The sucrose content was readjusted to <10% and the phagolysosomes concentrated by ultracentrifugation at $20{,}000\times g$ for 20 min, resuspended in isolation buffer, and frozen in aliquots.

Proton Transport Assays

Microsome acidification was assayed by measuring fluorescence quench of acridine orange (excitation at 485 nm and emission at 535 nm). Assays were performed in 96-well plates and measured with a Cameleon microplate reader (Hidex OY, Turku, Finland). The microplate reader was programmed to take fluorescence readings of the wells at 20-, 30-, or 120-second intervals. The assay mix consisted of 150 mM KCl, 5 mM $MgSO_4$, 1.5 μM acridine orange, 1 μM valinomycin, and 5 mM Tris/HEPES (pH 7.4). Inhibitors were added 20–30 min before the start of the assay in 2 μl DMSO, and control contained only DMSO. To start the tissue vesicle acidification, ATP was added to 5 mM from a 250-mM stock buffered to pH 7.4 with Tris. To dissipate the proton gradient at the end of the experiment, nigericin was added to a final concentration of 10 μg/ml. Phagolysosomes were acidified as with the tissue-derived microsomes, except that the assay volume was scaled down to 50 μl, the inhibitor was added in 1 μl DMSO, and the reaction was started with 2 mM ATP.

We noted that the amount of microsomes and phagolysosomes affected the IC_{50} [25]; therefore, we used amounts of microsomes and phagolysosomes that gave a clear quench of fluorescence and were partly inhibited by 0.3 nM bafilomycin A1, which was used as a reference inhibitor. Moreover, since at room temperature the acidification activity of all preparations decreased with time, the experiments were performed with both inhibitors simultaneously, and representative results are presented.

Results

Localization of the V-ATPase a3 Isoform in Resorbing Human Osteoclasts

We first examined whether a3 expression is induced in in vitro differentiated human osteoclasts. By immunofluorescence staining with an a3-specific antibody, multinucleated cells were heavily a3-positive while no or weak staining was detected in nondifferentiated mononuclear cells (Fig. 1a), showing that a3 expression is highly induced during osteoclast differentiation. When cultured on bovine cortical bone slices, the osteoclasts formed resorption pits. In such resorbing osteoclasts a3 was mainly localized within the actin ring (Fig. 1b), which delimits the ruffled border. Co-immunostaining of a3 and osteocalcin, a bone matrix protein, showed that a3 is polarized toward the leading edge of the pit, which is being resorbed (Fig. 1c), further supporting an important role for a3 in the resorption of bone mineral.

Subcellular Localization of the V-ATPase a3 Isoform

To identify the subcellular origin of a3 in nonresorbing osteoclasts, we co-immunostained osteoclasts cultured on glass coverslips. a3 was clearly localized to intracellular vesicular structures and colocalized almost perfectly with LAMP-2, a transmembrane glycoprotein involved in lysosomal maintenance and often used as a marker protein of lysosomes and late endosomes (Fig. 2a). Isoform a3 also partly colocalized with cathepsin K (Fig. 2b), a cystein proteinase highly expressed in osteoclasts and necessary for proper bone resorption [26]. As cathepsin K is secreted into the resorption lacuna [27], this vesicle population is likely to fuse with the ruffled border membrane. To investigate if a3 was present in other vesicular membranes, we stained the cells with an antibody specific for matrix metalloproteinase-9 (Fig. 2c), a nonlysosomal collagenase also important in bone resorption, and with an antibody specific for early endosomal antigen-1 (Fig. 2d). No colocalization of a3 was observed with either of these antigens, suggesting that a3 localization is limited to the late endosomal/lysosomal compartment in nonresorbing osteoclasts.

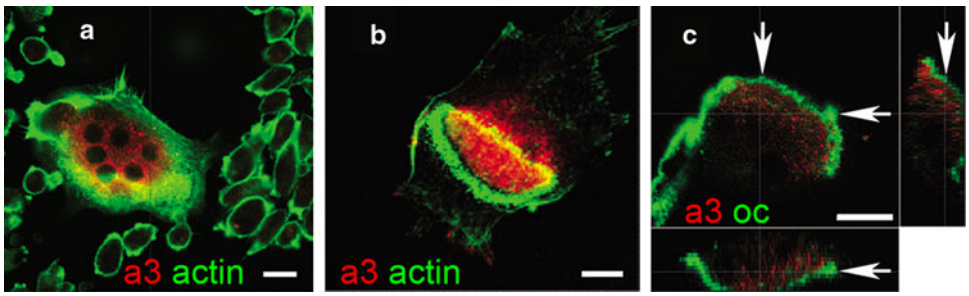

Fig. 1 Immunofluorescent images of in vitro differentiated osteoclasts cultured on bovine cortical bone slices. In comparison with nondifferentiated mononuclear cells, the a3 subunit of V-ATPase is highly upregulated in multinucleated osteoclasts (**a**). In actively resorbing osteoclasts, a3 localizes mainly within the actin ring (**b**). In osteoclasts associated with pits, the edges of which are visualized by osteocalcin (*oc*) staining, polarization of a3 toward the leading edge of the pit (*arrows*) is evident (**c**), especially from the *xz* and *yz* projections. In **a** and **b** the projection of all optical sections generated with confocal microscope is shown, and in **c** a 1-μm-thick optical section at the level of nuclei is shown together with *xz* and *yz* projections at the levels indicated by *arrows*. Bars = 10 μm

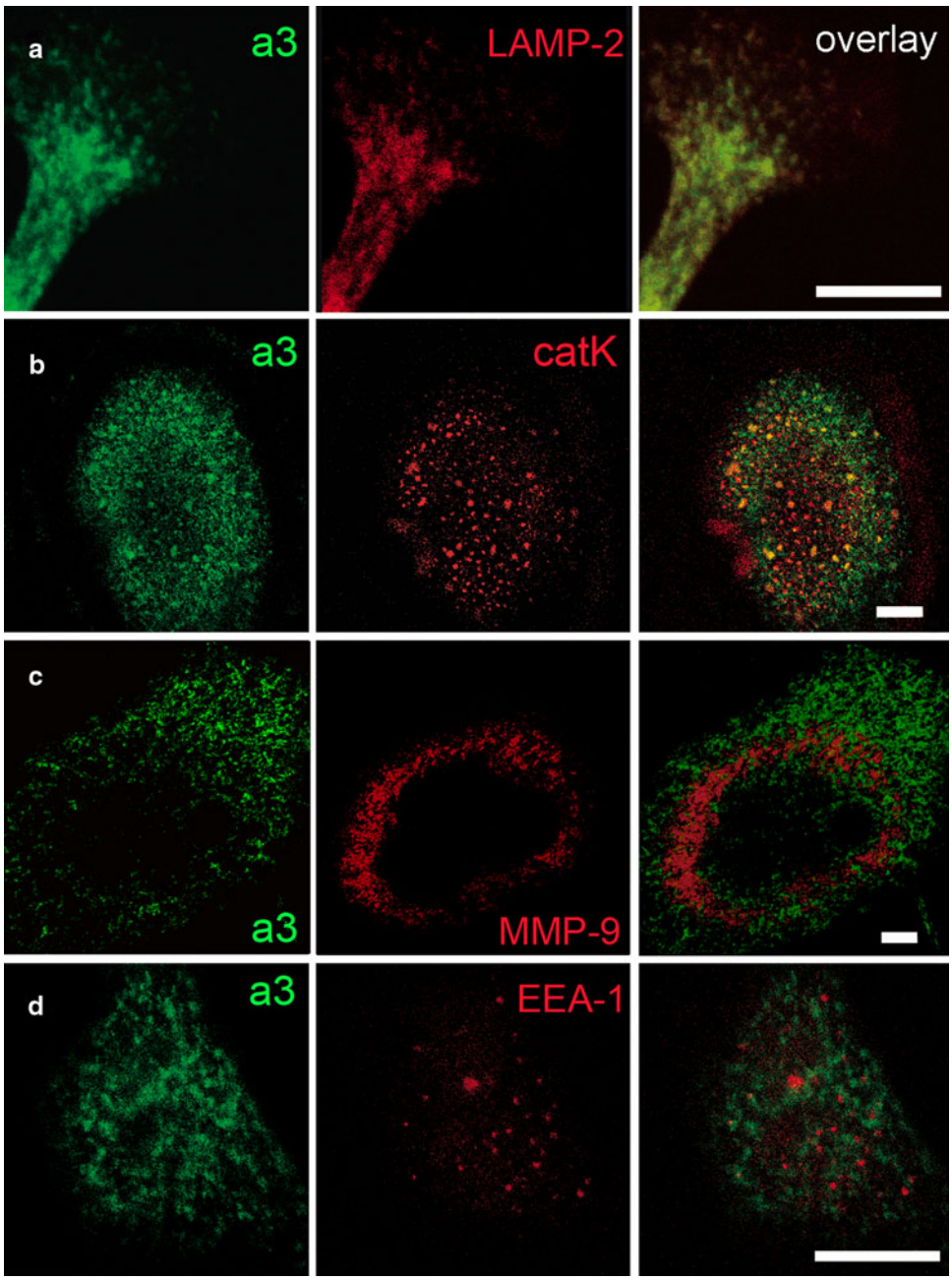

Fig. 2 The a3 subunit of V-ATPase is lysosomal in nonresorbing osteoclasts cultured on coverslips. a3 colocalizes almost completely with LAMP-2 (**a**) and extensively with cathepsin K (*catK*) (**b**). In contrast, the signals from a3-staining and metalloproteinase-9-staining (MMP-9) do not overlap; these antigens localize partly to different domains of the osteoclast (**c**). Early endosome antigen-1-positive (EEA-1) vesicles were observed close to a3-positive vesicles, but the signals for these antigens did not overlap (**d**). Shown are 1-µm-thick optical sections generated by confocal microscopy. Bars = 5 µm

Phagocytosis and Localization of Latex Beads in Osteoclasts

By immunostaining we failed to detect any specific a3 staining in the HeLa, PC3, MCF7, and THP.1 cell lines (not shown) and instead turned our focus on isolating the isoform a3-positive compartment from osteoclasts and comparing it to the corresponding compartment of another cell source. The lysosomal localization of a3 in osteoclasts suggested that this a3-positive compartment could be isolated as latex bead-containing phagolysosomes [28]. In vitro differentiated human osteoclasts in cell culture dishes readily phagocytosed latex beads (Fig. 3a). Resorbing osteoclasts on bone did not phagocytose latex beads (not shown), so a direct localization of the latex bead-containing phagolysosomes to the ruffled border area of resorbing osteoclasts could not be confirmed. However, when we added bone particles to osteoclasts on coverslips that already had phagocytosed latex beads, the phagolysosomes relocalized and concentrated to the vicinity of the bone particle in many osteoclasts (Fig. 3b). This event appeared to be actin-dependent since it was not observed in osteoclasts where bone particles were without associated actin-filament staining (Fig. 3c). In monocytic THP.1 cells, the

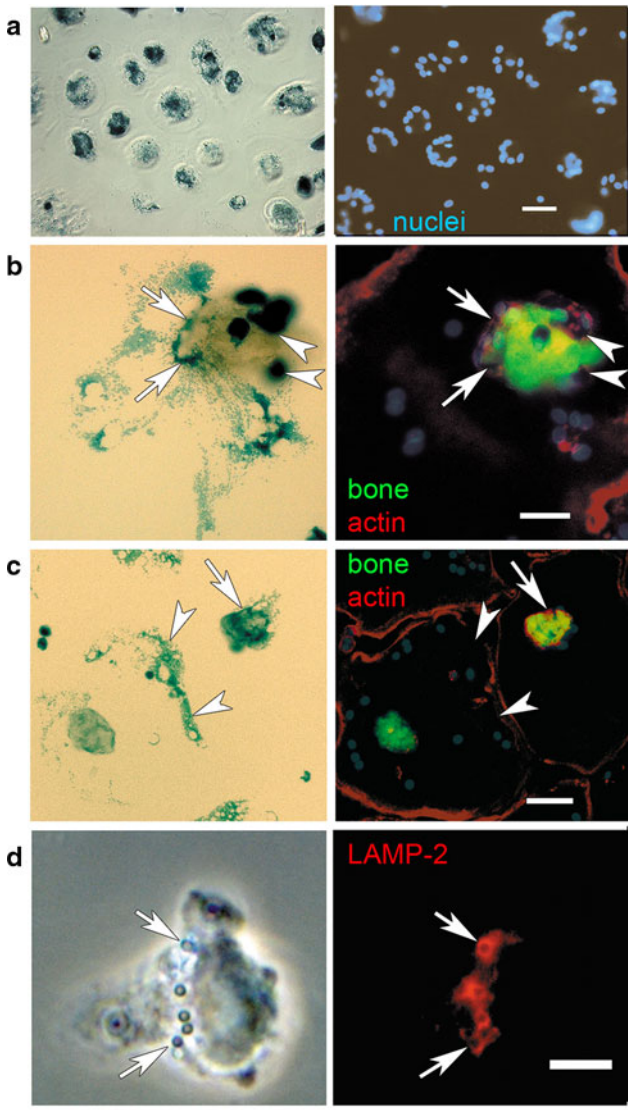

Fig. 3 Phagocytosis and localization of latex beads. **a** Blue-colored latex beads, visible by phase-contrast optics, are efficiently phagocytosed by human osteoclasts grown on coverslips. Cells were allowed to phagocytose latex beads for 4 h, after which nonphagocytosed beads were rinsed off and cells were incubated for 20 h before fixation and staining. **a** The purity of the cultures used for phagolysosome isolation; only a few of the latex bead-containing cells are mononuclear cells as shown with Hoechst staining. Bar = 50 μm. **b** Accumulations of latex bead-containing phagolysosomes (*arrows*) were frequently observed adjacent to subsequently added bone particles. In this experiment the cells were first allowed to phagocytose latex beads, washed, and incubated for 20 h; then, bone particles were added and the cells incubated for another 24 h before fixation and staining. *Arrowheads* indicate mononuclear cells on the bone particle. Bar = 40 μm. **c** Extensive relocalization of the latex bead-containing phagolysosomes to the vicinity of the bone particle was only observed in osteoclasts with extensive actin filament decoration of the bone particle (*arrow*). In osteoclasts with no actin staining associated with the bone particle the phagolysosomes were dispersed in the peri- and internuclear regions (*arrowheads*). Bar = 50 μm. **d** In monocytic THP.1 cells, the phagocytosed latex beads entered into the lysosomal compartment as evidenced by LAMP-2-positive delimiting membranes. Two latex beads are indicated by *arrows*. Bar = 5 μm. (Color figure online)

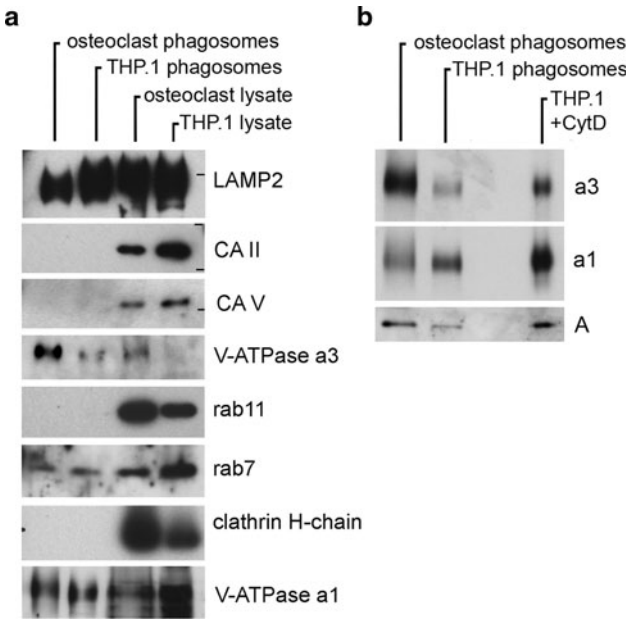

Fig. 4 **a** Characterization of phagolysosomal purity by immunoblotting. Aliquots of phagolysosomes isolated from osteoclasts and THP.1 cells, roughly equal to 10 μg of whole-cell lysates from osteoclast and THP.1 cultures with respect to LAMP-2 levels, were subjected to polyacrylamide gel electrophoresis; and the indicated antigens were immunoblotted. V-ATPase a3 and rab7 (a small GTP-binding protein involved in lysosomal biogenesis) were present in the phagosomal fractions, as was V-ATPase a1. The phagosomal fractions were essentially devoid of the nonlysosomal antigens tested: carbonic anhydrase II (CA II), carbonic anhydrase V (CA V), rab11, and the clathrin heavy chain. **b** Osteoclast phagolysosomes and THP.1 phagolysosomes are positive for both a3 and a1, but osteoclast phagolysosomes have a higher a3/a1 ratio. The A subunit level is also higher in osteoclast phagolysosomes. Cytochalasin D treatment 30 min before and during the isolation of phagolysosomes from THP.1 cells (THP.1 + CytD) did not affect a1, a3, or A levels

cell line that we chose for comparison, the phagocytosed latex beads clearly entered into the LAMP-2-positive compartment (Fig. 3d).

Characterization of Phagolysosomes Isolated from Osteoclasts and THP.1 Cells

We isolated phagolysosomes from osteoclast cultures and THP.1 cells and characterized them qualitatively by comparing their protein contents with the respective total cell lysates (Fig. 4a). In addition to LAMP-2, Rab7, a small GTPase involved in lysosomal biogenesis, was retained on both phagosomal fractions. Both phagosomal fractions were essentially depleted of the nonlysosomal proteins assayed: Rab11, which is a small GTPase located to recycling endosomes; cytosolic carbonic anhydrase II; mitochondrial carbonic anhydrase V; and the clathrin heavy chain, which is a component of coated pits and vesicles budding from the plasma membrane and the *trans*-Golgi network. Importantly,

a3 was clearly present in both phagolysosomal fractions; however, the a3 level was clearly higher in osteoclast phagosomes than in THP.1 phagosomes, and a3 was not clearly detectable in the THP.1 cell lysate. Unexpectedly, another isoform of the 116-kDa subunit, a1, which we used as a control for a3, was also present in both phagolysosomal fractions, even though it has not been associated with lysosomes or osteoclast function [9, 11, 13].

Relative Protein Levels of a3 and a1 on Phagolysosomes from Osteoclasts and THP.1 Cells

The coexistence of a3 and a1 on isolated phagolysosomes has a potential pharmacological impact and was characterized further. The size difference between a3 and a1 confirmed that the antisera did not cross-react (not shown). By quantification of a3 and a1 bands on immunoblots from three separate experiments (one representative is shown in Fig. 4b), we found that the a3/a1 ratio was 3.8- to 11.2-fold higher in osteoclast phagolysosomes (mean 6.9) than in THP.1 phagolysosomes. In addition, the protein levels of subunit A, a member of the cytosolic sector of V-ATPase, mirror a3 levels rather than a1 levels (Fig. 4b), indicating that the increased a3 levels on osteoclast phagolysosomes represent assembled V-ATPase, not only the membrane sector. Moreover, treatment with 20 μM cytochalasin D, a toxin that disrupts actin filaments, for 30 min before and during the isolation of phagolysosomes from THP.1 cells did not affect the a3 and a1 levels compared to untreated sample (Fig. 4b), indicating that V-ATPases are not associated with the phagolysosomes nonspecifically through actin filaments.

Acidification of Phagolysosomes from Osteoclasts and THP.1 Cells and Their Sensitivity to V-ATPase Inhibitors

To assess whether the V-ATPases of the isolated phagolysosomes show any difference in their sensitivity to inhibitors, we tested the SB242784 compound, which was successfully used to treat experimentally induced osteoporosis of the rat. This compound was reported to be selective for osteoclast V-ATPase in vivo, and in vitro fivefold selectivity for chicken osteoclast V-ATPase activity over chicken adrenal gland V-ATPase activity has been reported [4]. We first confirmed the selectivity of this compound on the chicken bone and brain-derived microsomes; in conditions where 0.3 and 1 nM bafilomycin A1 inhibited acidification of both sources by approximately 30% and 70–80%, respectively, SB242784 was approximately threefold less potent on brain-derived vesicles than on bone-derived microsomes (Fig. 5).

After minor modifications, the acidification assay protocol for microsomes could be applied with the isolated phagolysosomes, and the fluorescence quench increased with increasing amounts of phagolysosomes (not shown). One apparent difference when compared to the tissue-derived microsomes was that the acidification of phagolysosomes continued for a longer time before reaching a plateau. Osteoclast phagolysosomes acidified faster than THP.1 phagolysosomes (Fig. 6), a fact that may reflect the observed difference in V-ATPase levels between osteoclasts and THP.1 phagolysosomes (Fig. 4b). The acidification was dose-dependently sensitive to V-ATPase inhibitors within the same range of concentrations as the tissue-derived microsomes. When the amounts of phagolysosomes were adjusted so that 0.3 nM bafilomycin A1 inhibited approximately 50% of the acidification-mediated fluorescence quench, SB242784 at concentrations of 3, 10, and 30 nM inhibited both sources of phagolysosomes very similarly, although the relative sensitivity of osteoclast phagolysosomes to SB242784 appeared to be slightly higher (Fig. 6). This result shows that osteoclast phagolysosomal acidification is very sensitive to SB242784 and indicates that there is very little, if any, selectivity of SB242784 for the V-ATPase of osteoclast phagolysosomes over that of THP.1 phagolysosomes.

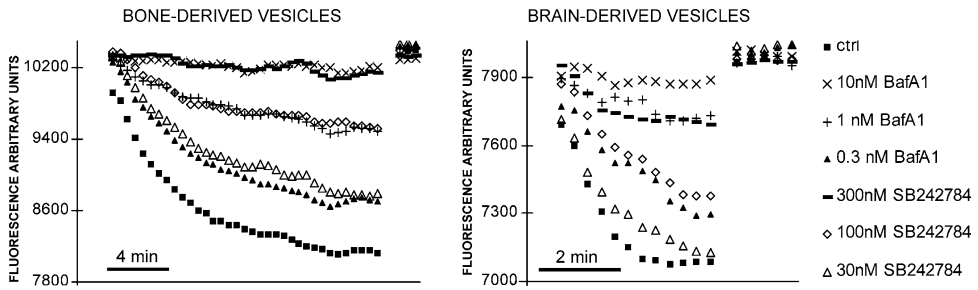

Fig. 5 Dose-dependent effects of the V-ATPase inhibitors bafilomycin A1 (BafA1) and SB242784 on the acidification of chicken bone- and brain-derived microsomes. The amounts of vesicles were adjusted so that half-maximal inhibition was reached by BafA1 at a concentration between 0.3 and 1 nM. In these conditions, for bone-derived vesicles, 30 nM SB242784 inhibited acidification equally to 0.3 nM BafA1 and 100 nM SB242784, equally to 1 nM BafA1. The brain-derived vesicles are less sensitive to SB242784; 100 nM SB242784 inhibited acidification equally to 0.3 nM BafA1 and 300 nM SB242784, equally to 1 nM BafA1

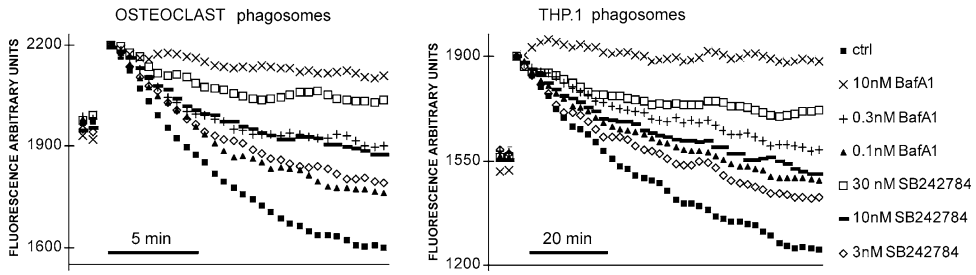

Fig. 6 Acidification of isolated phagolysosomes and the dose-dependent effects of bafilomycin A1 (BafA1) and SB242784 on acidification. The amount of phagolysosomes in the assays was adjusted so that fluorescence was quenched by 30–35%. In these conditions, phagolysosomes isolated from osteoclasts acidified faster than phagolysosomes from THP.1 cells and half-maximal inhibition was obtained with 0.3 nM bafilomycin A1. Phagolysosomes from osteoclasts are slightly more sensitive to SB242784 than phagolysosomes from THP.1 cells

Discussion

While it is well established that bone mineral dissolution by the osteoclast is mediated by V-ATPase activity [29, 30], it is not known how inhibitor selectivity for the osteoclast V-ATPase can be achieved. Although two structurally different V-ATPase inhibitors have shown promising performance in preclinical models of osteoporosis [7, 31, 32], in principle validating the target, the structural basis for selective inhibition is yet missing. The phenotype of a3-deficient mice suggested that a3 is a key mediator of selectivity.

To start with, we studied the localization of the a3 isoform in human osteoclasts. We found that a3, which in actively resorbing human osteoclasts was polarized toward the ruffled border area, colocalized with the lysosomal marker LAMP-2 and partly with cathepsin K in nonresorbing osteoclasts (Fig. 2a, b). This is in full agreement with the results of Toyomura et al. [11], who studied the localization of a3 in the murine RAW cell line and osteoclasts induced therefrom. It has been suggested that one of the roles of the "a" subunit is to target the V-ATPase to a specific compartment. In yeast, the two "a" homologues mediate targeting of the V-ATPase to different subcellular compartments [33, 34], and in mammals the isoforms localize to different subcellular compartments [11]. However, in addition to its lysosomal localization, a3 has been demonstrated in the membrane of insulin-containing secretory granules of pancreatic β-cells [35]. We observed no colocalization of a3 with early endosome antigen-1 or with matrix metalloproteinase-9 (Fig. 2c, d). This does not exclude low levels of a3 in these nonlysosomal organelles. However, we can conclude that the bulk of the a3 protein in osteoclasts is localized to LAMP-2-positive lysosomes/late endosomes in human osteoclasts. Therefore, we suggest that in resorbing osteoclasts this vesicle population is the main contributor to the acidification of the resorption lacuna. Using latex beads, we were successful in isolating the LAMP-2- and a3-positive compartment (Fig. 4), which possessed V-ATPase-mediated acidification (Fig. 6). Three independent facts suggest that the phagolysosomal V-ATPase represents the ruffled border V-ATPase. First, the high level of a3 expression in the osteoclast was represented on the isolated phagolysosomes (Fig. 4). Second, in living osteoclasts, the latex bead-containing phagolysosomes were transported to the close vicinity of subsequently added bone particles (Fig. 3b, c), mimicking the polarization of a3 in the resorbing osteoclast. Third, acidification of isolated phagolysosomes was highly sensitive to the SB242784 compound; in fact, the relative sensitivity to SB242784 was higher for osteoclast phagolysosomes than for microsomes derived from chicken bone. However, we isolated the phagolysosomes from nonresorbing osteoclasts, and we cannot exclude the possibility that some changes to the V-ATPase may occur upon activation of bone resorption.

Taken together, our data support the view that the ruffled border is mainly lysosomal in origin; i.e., the ruffled border is formed by the fusion of lysosomes with the plasma membrane [36]. Accordingly, the osteoclast ruffled border V-ATPase may be a common lysosomal V-ATPase that is only quantitatively upregulated, or it may possess a qualitatively unique subunit composition. The methodology we used allowed us to compare the a3-positive compartment from osteoclasts with the corresponding compartment from monocytic THP.1 cells. In this comparison, we found that phagolysosomes from THP.1 cells also contained the a3 isoform (Fig. 4), although significantly less than did osteoclast phagolysosomes, and that the SB242784 compound inhibited acidification of the isolated phagolysosomes from both sources at similar concentrations (Fig. 6). We believe that the small difference in relative sensitivity to SB242784 between osteoclasts and THP.1 phagolysosomes (Fig. 6) is due to the differential a3/a1 ratios (Fig. 4), rather than representing a true pharmacological difference. Thus, we have no indication of a qualitative difference between the V-ATPases from the two sources. Rather than indicating something unique, the high level of a3 expression in the

osteoclast and its phagolysosomes may represent the fact that a high level of lysosomal V-ATPase is needed for efficient bone resorption, while significantly less V-ATPase is needed to maintain lysosomal pH in other cells. Nevertheless, the osteoclast lysosomal V-ATPase may possess qualitative differences in other subunits, which we were not able to address here, due to the lack of isoform-specific antibodies. Of particular interest may be the d2 isoform, which, in contrast to d1, has limited tissue expression including osteoclast, kidney, and lung [37]. Recently, d2 was reported to directly interact with a3 in osteoclasts [38]. It remains to be found out whether this interaction is limited to osteoclasts. As far as we are aware, there are only few data indicating that the osteoclast ruffled border V-ATPase is pharmacologically distinguishable from the lysosomal V-ATPase; Niikura et al. [31, 32] reported a V-ATPase inhibitor that was sevenfold less potent on liver lysosomal V-ATPase than on osteoclast V-ATPase, although a3 mRNA is expressed at a high level in liver [8, 9, 13, 39].

The most interesting finding, which needs to be followed up for reasons discussed below, was the presence of the a1 isoform on the phagolysosomes. This observation was surprising because a1 was originally found in clathrin-coated vesicles [40]. However, by immunostaining, there was some colocalization of a1 with LAMP1, although the bulk did not colocalize [11]. Recently, a1 was found as a component of late endosomes by proteomic analysis [41]. It must be considered that the organelles are not static structures; transient but frequent membrane trafficking events are also represented by the phagolysosomes. Nonetheless, the identification of a3 and a1 in model phagolysosomes is the first piece of evidence for a compensation of a3, the concept discussed by Manolson et al. [13]. Compensation would explain why a3-deficient patients do not have any lysosomal defect [42], as would be expected if a3 was the only isoform in this compartment. It would also explain why there is some residual bone resorption left in a3-defective osteoclasts [43, 44]. Evidence of at least a partial functional compensation of a3 by another V-ATPase comes from macrophages from mice with a disrupted gene for a3, which acidified phagosomes by a bafilomycin-sensitive mechanism [45]. Moreover, these cells had normal levels of mature cathepsins and were capable of bacterial killing, albeit at a significantly slower rate than control macrophages [45].

From the pharmacological point of view, the presence of a compensating "a" isoform in the lysosome would also provide a rationale for osteoclast selectivity of an a3-selective inhibitor; inhibition of a3 would not affect basal lysosomal function if it can be sufficiently maintained by another V-ATPase. Osteoclasts, on the contrary, need a high level of V-ATPase for bone resorption, and such a compensatory mechanism is not sufficient for proper bone resorption. The outcome of V-ATPase a3-selective inhibition would then be as bone-specific as is a3 deficiency. To further elucidate the putative compensation of a3 by other isoforms, it would be instructing to isolate and analyze phagolysosomes from a3-deficient cells with respect to the acidifying properties.

The selectivity of SB242784 between tissue-derived microsomes may be explained by the reported differential expression levels of "a" isoforms; the bone tissue possessing the highest level of a3 being most sensitive [13, 39]. Isoform a3 selectivity may be a very important property of SB242784 in limiting the inhibition to the lysosomal V-ATPase, including the osteoclast ruffled border. The compensating mechanism may then protect the lysosomal function, leaving the osteoclast ruffled border V-ATPase most sensitive to inhibition. However, because the selectivity of SB242784 is only three- to fivefold, we doubt that the compensating mechanism operates at its full capacity, and the efficacy of SB242784 in rat models of osteoporosis [7, 32] may not be due only to this mechanism. We believe that additional mechanisms that favor osteoclast inhibition over inhibition of lysosomal functions may exist in vivo. Specifically, we speculate that lysosomes and lysosomal enzymes may possess an overcapacity while the ruffled border V-ATPase, on the other hand, is rate-limiting for bone resorption. As a consequence of this difference, submaximal inhibition of V-ATPase could have a dramatic impact on bone resorption with little impact on lysosomal function. Further studies are required to address the contribution of such mechanisms.

In conclusion, a3 in osteoclasts is lysosomal, and this a3-positive compartment can be isolated as phagolysosomes. However, a3 was also present in phagolysosomes from the THP.1 cell line, and the acidification of these isolated phagolysosomes was essentially equally sensitive to SB242784. Thus, if existing, a unique structural feature of the osteoclast V-ATPase that would allow its selective targeting remains to be identified. However, the presence of multiple "a" isoforms in the model phagolysosomes suggests that a3, despite its reported ubiquitous expression, is a valid drug target since other functions than bone resorption may be compensated.

Acknowledgements This work was funded from the European Commission under contract QLG-CT-2000-01801 (MIVase-New Therapeutic Approaches to Osteoporosis, targeting the osteoclast V-ATPase). Dr. Kalman Büki is acknowledged for critical reading of the manuscript.

References

1. Palokangas H, Mulari M, Vaananen HK (1997) Endocytic pathway from the basal plasma membrane to the ruffled border membrane in bone-resorbing osteoclasts. J Cell Sci 110 (Pt 15): 1767–1780

2. Nishi T, Forgac M (2002) The vacuolar H^+-ATPases—nature's most versatile proton pumps. Nat Rev Mol Cell Biol 3:94–103
3. Keeling DJ, Herslof M, Ryberg B, Sjogren S, Solvell L (1997) Vacuolar H^+-ATPases. Targets for drug discovery? Ann N Y Acad Sci 834:600–608
4. Nadler G, Morvan M, Delimoge I, Belfiore P, Zocchetti A, James I, Zembryki D, Lee-Rycakzewski E, Parini C, Consolandi E, Gagliardi S, Farina C (1998) (2Z, 4E)-5-(5,6-Dichloro-2-indolyl)-2-methoxy-N-(1,2,2,6,6-pentamethylpiperidin-4-yl)-2,4-pentadienamide, a novel, potent and selective inhibitor of the osteoclast V-ATPase. Bioorg Med Chem Lett 8:3621–3626
5. Gagliardi S, Rees M, Farina C (1999) Chemistry and structure activity relationships of bafilomycin A1, a potent and selective inhibitor of the vacuolar H^+-ATPase. Curr Med Chem 6:1197–1212
6. Gagliardi S, Nadler G, Consolandi E, Parini C, Morvan M, Legave MN, Belfiore P, Zocchetti A, Clarke GD, James I, Nambi P, Gowen M, Farina C (1998) 5-(5,6-Dichloro-2-indolyl)-2-methoxy-2,4-pentadienamides: novel and selective inhibitors of the vacuolar H^+-ATPase of osteoclasts with bone antiresorptive activity. J Med Chem 41:1568–1573
7. Visentin L, Dodds RA, Valente M, Misiano P, Bradbeer JN, Oneta S, Liang X, Gowen M, Farina C (2000) A selective inhibitor of the osteoclastic V-H^+-ATPase prevents bone loss in both thyroparathyroidectomized and ovariectomized rats. J Clin Invest 106:309–318
8. Nishi T, Forgac M (2000) Molecular cloning and expression of three isoforms of the 100-kDa a subunit of the mouse vacuolar proton-translocating ATPase. J Biol Chem 275:6824–6830
9. Toyomura T, Oka T, Yamaguchi C, Wada Y, Futai M (2000) Three subunit a isoforms of mouse vacuolar H^+-ATPase. Preferential expression of the a3 isoform during osteoclast differentiation. J Biol Chem 275:8760–8765
10. Oka T, Murata Y, Namba M, Yoshimizu T, Toyomura T, Yamamoto A, Sun-Wada GH, Hamasaki N, Wada Y, Futai M (2001) a4, a unique kidney-specific isoform of mouse vacuolar H^+-ATPase subunit a. J Biol Chem 276:40050–40054
11. Toyomura T, Murata Y, Yamamoto A, Oka T, Sun-Wada GH, Wada Y, Futai M (2003) From lysosomes to the plasma membrane: localization of vacuolar-type H^+-ATPase with the a3 isoform during osteoclast differentiation. J Biol Chem 278:22023–22030
12. Dou H, Xu J, Wang Z, Smith AN, Soleimani M, Karet FE, Greinwald JH Jr, Choo D (2004) Co-expression of pendrin, vacuolar H^+-ATPase alpha4-subunit and carbonic anhydrase II in epithelial cells of the murine endolymphatic sac. J Histochem Cytochem 52:1377–1384
13. Manolson MF, Yu H, Chen W, Yao Y, Li K, Lees RL, Heersche JN (2003) The a3 isoform of the 100-kDa V-ATPase subunit is highly but differentially expressed in large ($\geq$10 nuclei) and small ($\leq$nuclei) osteoclasts. J Biol Chem 278:49271–49278
14. Li YP, Chen W, Liang Y, Li E, Stashenko P (1999) Atp6i-deficient mice exhibit severe osteopetrosis due to loss of osteoclast-mediated extracellular acidification. Nat Genet 23:447–451
15. Frattini A, Orchard PJ, Sobacchi C, Giliani S, Abinun M, Mattsson JP, Keeling DJ, Andersson AK, Wallbrandt P, Zecca L, Notarangelo LD, Vezzoni P, Villa A (2000) Defects in TCIRG1 subunit of the vacuolar proton pump are responsible for a subset of human autosomal recessive osteopetrosis. Nat Genet 25:343–346
16. Kornak U, Schulz A, Friedrich W, Uhlhaas S, Kremens B, Voit T, Hasan C, Bode U, Jentsch TJ, Kubisch C (2000) Mutations in the a3 subunit of the vacuolar H^+-ATPase cause infantile malignant osteopetrosis. Hum Mol Genet 9:2059–2063
17. Sobacchi C, Frattini A, Orchard P, Porras O, Tezcan I, Andolina M, Babul-Hirji R, Baric I, Canham N, Chitayat D, Dupuis-Girod S, Ellis I, Etzioni A, Fasth A, Fisher A, Gerritsen B, Gulino V, Horwitz E, Klamroth V, Lanino E, Mirolo M, Musio A, Matthijs G, Nonomaya S, Notarangelo LD, Ochs HD, Superti Furga A, Valiaho J, van Hove JL, Vihinen M, Vujic D, Vezzoni P, Villa A (2001) The mutational spectrum of human malignant autosomal recessive osteopetrosis. Hum Mol Genet 10:1767–1773
18. Michigami T, Kageyama T, Satomura K, Shima M, Yamaoka K, Nakayama M, Ozono K (2002) Novel mutations in the a3 subunit of vacuolar H^+-adenosine triphosphatase in a Japanese patient with infantile malignant osteopetrosis. Bone 30:436–439
19. Scott BB, Chapman CG (1998) The putative 116 kDa osteoclast specific vacuolar proton pump subunit has ubiquitous tissue distribution. Eur J Pharmacol 346:R3–R4
20. Husheem M, Nyman JK, Vaaraniemi J, Vaananen HK, Hentunen TA (2005) Characterization of circulating human osteoclast progenitors: development of in vitro resorption assay. Calcif Tissue Int 76:222–230
21. Hellman J, Kakonen SM, Matikainen MT, Karp M, Lovgren T, Vaananen HK, Pettersson K (1996) Epitope mapping of nine monoclonal antibodies against osteocalcin: combinations into two-site assays affect both assay specificity and sample stability. J Bone Miner Res 11:1165–1175
22. Vaananen HK, Parvinen EK (1983) High active isoenzyme of carbonic anhydrase in rat calvaria osteoclasts. Immunohistochemical study. Histochemistry 78:481–485
23. Vaananen HK, Carter ND, Dodgson SJ (1991) Immunocytochemical localization of mitochondrial carbonic anhydrase in rat tissues. J Histochem Cytochem 39:451–459
24. Desjardins M, Huber LA, Parton RG, Griffiths G (1994) Biogenesis of phagolysosomes proceeds through a sequential series of interactions with the endocytic apparatus. J Cell Biol 124:677–688
25. Mattsson JP, Lorentzon P, Wallmark B, Keeling DJ (1993) Characterization of proton transport in bone-derived membrane vesicles. Biochim Biophys Acta 1146:106–112
26. Gelb BD, Shi GP, Chapman HA, Desnick RJ (1996) Pycnodysostosis, a lysosomal disease caused by cathepsin K deficiency. Science 273:1236–1238
27. Xia L, Kilb J, Wex H, Li Z, Lipyansky A, Breuil V, Stein L, Palmer JT, Dempster DW, Bromme D (1999) Localization of rat cathepsin K in osteoclasts and resorption pits: inhibition of bone resorption and cathepsin K-activity by peptidyl vinyl sulfones. Biol Chem 380:679–687
28. Sakai E, Miyamoto H, Okamoto K, Kato Y, Yamamoto K, Sakai H (2001) Characterization of phagosomal subpopulations along endocytic routes in osteoclasts and macrophages. J Biochem 130:823–831
29. Blair HC, Teitelbaum SL, Ghiselli R, Gluck S (1989) Osteoclastic bone resorption by a polarized vacuolar proton pump. Science 245:855–857
30. Vaananen HK, Karhukorpi EK, Sundquist K, Wallmark B, Roininen I, Hentunen T, Tuukkanen J, Lakkakorpi P (1990) Evidence for the presence of a proton pump of the vacuolar H^+-ATPase type in the ruffled borders of osteoclasts. J Cell Biol 111:1305–1311
31. Niikura K, Takano M, Sawada M (2004) A novel inhibitor of vacuolar ATPase, FR167356, which can discriminate between osteoclast vacuolar ATPase and lysosomal vacuolar ATPase. Br J Pharmacol 142:558–566
32. Niikura K, Takeshita N, Takano M (2005) A vacuolar ATPase inhibitor, FR167356, prevents bone resorption in ovariectomized rats with high potency and specificity: potential for clinical application. J Bone Miner Res 20:1579–1588
33. Manolson MF, Wu B, Proteau D, Taillon BE, Roberts BT, Hoyt MA, Jones EW (1994) STV1 gene encodes functional homologue of 95-kDa yeast vacuolar H^+-ATPase subunit Vph1p. J Biol Chem 269:14064–14074
34. Kawasaki-Nishi S, Bowers K, Nishi T, Forgac M, Stevens TH (2001) The amino-terminal domain of the vacuolar proton-translocating

ATPase a subunit controls targeting and in vivo dissociation, and the carboxyl-terminal domain affects coupling of proton transport and ATP hydrolysis. J Biol Chem 276:47411–47420
35. Sun-Wada GH, Toyomura T, Murata Y, Yamamoto A, Futai M, Wada Y (2006) The a3 isoform of V-ATPase regulates insulin secretion from pancreatic beta-cells. J Cell Sci 119:4531–4540
36. Stenbeck G (2002) Formation and function of the ruffled border in osteoclasts. Semin Cell Dev Biol 13:285–292
37. Smith AN, Borthwick KJ, Karet FE (2002) Molecular cloning and characterization of novel tissue-specific isoforms of the human vacuolar H^+-ATPase C, G, and d subunits, and their evaluation in autosomal recessive distal renal tubular acidosis. Gene 297:169–177
38. Wu H, Xu G, Li YP (2009) Atp6v0d2 is an essential component of the osteoclast-specific proton pump that mediates extracellular acidification in bone resorption. J Bone Miner Res 24:871–885
39. Mattsson JP, Li X, Peng SB, Nilsson F, Andersen P, Lundberg LG, Stone DK, Keeling DJ (2000) Properties of three isoforms of the 116-kDa subunit of vacuolar H^+-ATPase from a single vertebrate species. Cloning, gene expression and protein characterization of functionally distinct isoforms in *Gallus gallus*. Eur J Biochem 267:4115–4126
40. Perin MS, Fried VA, Stone DK, Xie XS, Sudhof TC (1991) Structure of the 116-kDa polypeptide of the clathrin-coated vesicle/synaptic vesicle proton pump. J Biol Chem 266: 3877–3881
41. Lafourcade C, Sobo K, Kieffer-Jaquinod S, Garin J, van der Goot FG (2008) Regulation of the V-ATPase along the endocytic pathway occurs through reversible subunit association and membrane localization. PLoS One 3:e2758
42. Blair HC, Borysenko CW, Villa A, Schlesinger PH, Kalla SE, Yaroslavskiy BB, Garcia-Palacios V, Oakley JI, Orchard PJ (2004) In vitro differentiation of CD14 cells from osteopetrotic subjects: contrasting phenotypes with TCIRG1, CLCN7, and attachment defects. J Bone Miner Res 19:1329–1338
43. Taranta A, Migliaccio S, Recchia I, Caniglia M, Luciani M, De Rossi G, Dionisi-Vici C, Pinto RM, Francalanci P, Boldrini R, Lanino E, Dini G, Morreale G, Ralston SH, Villa A, Vezzoni P, Del Principe D, Cassiani F, Palumbo G, Teti A (2003) Genotype–phenotype relationship in human ATP6i-dependent autosomal recessive osteopetrosis. Am J Pathol 162:57–68
44. Del Fattore A, Peruzzi B, Rucci N, Recchia I, Cappariello A, Longo M, Fortunati D, Ballanti P, Iacobini M, Luciani M, Devito R, Pinto R, Caniglia M, Lanino E, Messina C, Cesaro S, Letizia C, Bianchini G, Fryssira H, Grabowski P, Shaw N, Bishop N, Hughes D, Kapur RP, Datta HK, Taranta A, Fornari R, Migliaccio S, Teti A (2006) Clinical, genetic, and cellular analysis of 49 osteopetrotic patients: implications for diagnosis and treatment. J Med Genet 43:315–325
45. Sun-Wada GH, Tabata H, Kawamura N, Aoyama M, Wada Y (2009) Direct recruitment of H^+-ATPase from lysosomes for phagosomal acidification. J Cell Sci 122:2504–2513